Eigenmodes of a Symmetric Cylindrical Confocal Laser Resonator and Their Perturbation by Output-Coupling Apertures

By D. E. McCUMBER

(Manuscript received October 26, 1964)

Using a numerical technique which is different from the iteration method of Fox and Li and which is more suitable for the analysis of high-order modes, we have calculated the diffraction losses and the field distributions at the reflectors of the low-loss modes of a symmetric confocal resonator for Fresnel numbers $0.6 \leqq N_m \leqq 2.0$. *We have also computed the modifications which result when the two end reflectors are perturbed by circular output-coupling apertures centered on the cavity axis. For a range of small but useful aperture Fresnel numbers* N_0 *the aperture diffraction losses can be estimated by first-order perturbation theory from the finite-*N_m *results appropriate to* $N_0 = 0$. *Such estimates fail for those larger Fresnel numbers* N_0 *for which the mode intensity patterns are significantly distorted at the reflectors by the finite coupling apertures.*

I. INTRODUCTION

Fox and Li[1] demonstrated by numerical iteration that modes in the sense of self-reproducing field patterns exist for open Fabry-Perot resonators. Using a numerical technique which is different from that of Fox and Li and which is more suitable tban iteration for the analysis of high-order modes, we have calculated the diffraction losses and the field distributions at the reflectors of the low-loss modes of a symmetric cylindrical confocal resonator for Fresnel numbers $0.6 \leqq N_m \leqq 2.0$. The results are discussed below.

An axial section of the symmetric confocal resonator under examination is illustrated in Fig. 1. The cavity is bounded at each end by identical spherical (parabolic) mirrors whose perfectly reflecting surfaces extend over the annular region $a_0 \leqq \rho \leqq a_m$. While a comparison of

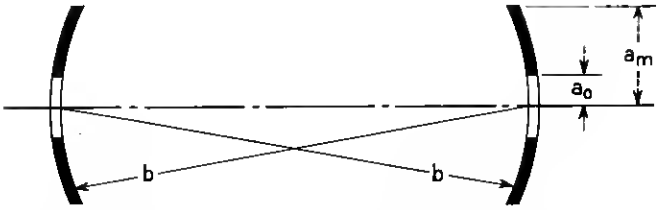

Fig. 1 — Axial section of cylindrical confocal laser cavity. The system is symmetric about the cavity midpoint; the two identical reflectors have radii of curvature b; and the reflecting surfaces are confined to the annular region between the two radii (a_0 , a_m).

the $a_0 = 0$ and $a_0 \neq 0$ eigenmodes is instructive as an example of the perturbation of eigenmodes by mirror imperfections, this particular geometry also has relevance to an aperture output coupling scheme proposed by Patel et al.[2] Asymmetric resonators in which, for example, only one reflector is pierced by a coupling aperture will be treated in a subsequent article. Boyd and Gordon[3] have derived closed-form expressions for the eigenvalues and eigenfunctions of symmetric *rectangular* confocal resonators in terms of the angular and radial prolate spheroidal wave functions. These results were extended to asymmetric rectangular confocal systems with output coupling *slits* by Boyd and Kogelnik.[4] Generalized prolate spheroidal functions relevant to the cylindrical confocal geometry have been defined by Slepian.[5] Basic expressions are summarized in a review article by Kogelnik.[6]

Assuming that the dimensions of the resonator in Fig. 1 are large compared to the wavelength λ of light in the cavity, we define the resonator eigenmodes from the same scalar formulation of Huygens' principle used by other authors.[1,3] For the cylindrical confocal geometry the field amplitude at the reflectors for a typical mode can be written in the form

$$F_{lp}(\rho,\varphi) = f_{lp}(\rho) \exp\ (-il\varphi), \tag{1}$$

where (ρ,φ) are radial and angular coordinates in a plane perpendicular to the resonator axis and where (l,p) are integral quantum numbers. For a symmetric system with identical mirrors, the field amplitude at one reflector must be a constant multiple of that at the other. This self-reproducing requirement together with Huygens' principle gives the following integral equation which must be satisfied by the radial function $f_{lp}(\rho)$:

$$\kappa_{lp} f_{lp}(\rho) = \frac{2\pi}{b\lambda} \int_{a_0}^{a_m} d\rho' \rho' J_l \left(\frac{2\pi\rho\rho'}{b\lambda}\right) f_{lp}(\rho'). \tag{2}$$

Here $J_l(z)$ is the Bessel function of order $|\,l\,|$, (a_0, a_m) are the ρ radii limiting the reflecting surfaces (Fig. 1), and b is the mirror separation and radius of curvature.

The magnitude of the eigenvalue κ_{lp} determines the diffraction loss of the (lp) mode:

$$\text{power loss/pass} = 1 - |\,\kappa_{lp}\,|^2. \tag{3}$$

The phase of the eigenvalue determines the resonant wavelength:

$$\text{resonant } \lambda = 4\pi b\{(l+1)\pi - 2\,\text{Arg}\,\kappa_{lp} - 2\pi n\}^{-1}, \tag{4}$$

where n is an arbitrary integer.

If we normalize the functions $f_{lp}(\rho)$ over the surface area of the mirrors, then

$$\frac{2\pi}{b\lambda}\int_{a_0}^{a_m} d\rho\,\rho f_{lp}(\rho) f_{lq}(\rho) = \delta_{pq}, \tag{5}$$

where δ_{pq} is the Kronecker delta symbol ($\delta_{pq} = 1$ if $p = q$, and $\delta_{pq} = 0$ if $p \neq q$). The orthogonality indicated in (5) for $p \neq q$ follows immediately from (2) when the eigenvalues κ_{lp}, κ_{lq} are nondegenerate and can be imposed if they are degenerate. We choose the arbitrary sign of the function $f_{lp}(\rho)$ such that $f_{lp}(0^+) > 0$.

For numerical calculations it is useful to replace the radial variable ρ by a dimensionless variable r defined such that

$$N(\rho) \equiv r^2 \equiv \rho^2/\lambda b \tag{6}$$

is the Fresnel number appropriate to the radius ρ. We characterize the hole and mirror radii (a_0, a_m) by Fresnel numbers

$$N_0 = r_0^2 = \frac{a_0^2}{\lambda b}, \qquad N_m = r_m^2 = \frac{a_m^2}{\lambda b}. \tag{7}$$

In place of the function $f_{lp}(\rho)$ we introduce a function

$$g_{lp}(r) = f_{lp}(r\sqrt{\lambda b}) \tag{8}$$

for which (2) and (5) become:

$$\kappa_{lp} g_{lp}(r) = 2\pi \int_{r_0}^{r_m} dr'\, r' J_l(2\pi r r') g_{lp}(r'); \tag{9}$$

$$\delta_{pq} = 2\pi \int_{r_0}^{r_m} dr\, r g_{lp}(r) g_{lq}(r). \tag{10}$$

The sign convention $f_p(0^+) > 0$ requires $g_{lp}(0^+) > 0$.

The eigenvalue equation (9) for the confocal geometry is atypical

in the sense that it can he transformed to an equation having a Hermitian kernel: $2\pi(rr')^{\frac{1}{2}}J_l(2\pi rr')$. This fact implies that the eigenvalues κ_{lp} are real and that the largest eigenvalue (characteristic of the mode with lowest loss) can be computed by a variational method. These two features do not obtain in other laser geometries for which the integral-equation kernel is generally symmetric but not real — that is, not Hermitian.[7] While we do therefore expect some qualitative differences between the properties of confocal and nonconfocal geometries, we can infer from the work of Fox and Li[1] and other authors[8,9] that many features are similar. Both the iterative technique of Fox and Li and the kernel-expansion-truncation technique we describe below can be applied to nonconfocal as well as confocal systems.

If we assume that the set of functions $g_{lp}(r)$ is complete, we can understand the iterative method of Fox and Li as follows. Given an arbitrary initial field amplitude $g^{(0)}(r)$, we express it in the form

$$g^{(0)}(r) = \Sigma_p C_p g_{lp}(r). \tag{11}$$

Substituting this expression into the right-hand side of (9), we obtain on the left-hand side

$$g^{(1)}(r) = \Sigma_p C_p \kappa_{lp} g_{lp}(r),$$

the field amplitude after one transit of the optical cavity. Using this function on the right-hand side of (9) and repeating this iterative procedure, we obtain after n iterations

$$g^{(n)}(r) = \Sigma_p C_p \kappa_{lp}{}^n g_{lp}(r), \tag{12}$$

the field amplitude after n transits. In the limit of large n only terms belonging to the eigenvalue of largest magnitude represented ($C_p \neq 0$) on the right-hand side of (11) will remain. All other terms will be reduced in proportion to $(|\kappa_{lp}|/|\kappa_{lp}|_{\max})^n$. If the two largest eigenvalues are sufficiently different, this procedure conveniently yields for each angular quantum number l the eigenvalue of largest magnitude, the eigenvalue of second-largest magnitude (through the rate of convergence of the iteration), and the two amplitude functions belonging to these eigenvalues. Results for the cylindrical confocal resonator are given by Fox and Li.[1]

In our analysis of (9) we have chosen to apply a different technique from that outlined above. Briefly, we expand the Bessel-function kernel in (9) as a power series

$$J_l(z) = \left(\frac{z}{2}\right)^l \sum_{m=1}^{\infty} \frac{(-1)^{m-1}}{(m+l-1)!(m-1)!} \left(\frac{z}{2}\right)^{2(m-1)}, \tag{13}$$

truncate the series after a finite number M of terms, and reduce the integral eigenvalue equation (9) to an M-dimensional-matrix eigenvalue equation which we can easily solve numerically with standard matrix-diagonalization routines. [The reduction of (9) to a matrix equation is described in the Appendix.] A similar technique has been used for the plane cylindrical geometry by She and Heffner.[8] For the confocal system for which real-number algebra is sufficient, our computations require slightly less computer time than the iterative method. Moreover, they give the eigenvalues and eigenfunctions of higher-order modes, whereas for each l the iterative scheme of Fox and Li is practical only for the two largest eigenvalues and their amplitude functions.

Related methods have been utilized in limited calculations by other authors.[9, 10] In place of the power-series expansion (13) it has been suggested[10] that one utilize an expansion in associated Laguerre functions. Because the associated Laguerre functions are the exact eigenfunctions of the infinite-mirror problem ($a_0 = 0$, $a_m = \infty$), one might expect that fewer terms are required than for the power-series expansion (13) and that one can thereby simplify the solution of the matrix eigenvalue equation. While such considerations may indeed be relevant for Fresnel numbers so large that the matrix eigenvalue problem based upon (13) becomes prohibitive, the advantages are largely offset for small Fresnel numbers ($N_m \lesssim 4$) by the increased effort required to compute the necessary overlap integrals. A similar remark applies to the Fourier-Bessel expansion used for the plane cylindrical geometry by Bergstein and Schachter.[9]

One other numerical technique, different from both the iterative and the expansion-truncation techniques, deserves brief mention. If one approximates the integral in (9) by a sum over small but finite radial intervals, one has in effect reduced the integral equation to a matrix eigenvalue equation. If the number of intervals is not too large ($\lesssim 50$) it is practical to solve this problem directly, although for small Fresnel numbers considerably less effort is required with the iteration or expansion-truncation techniques.

In the following section we present results appropriate to the symmetric cylindrical confocal geometry in the absence of coupling apertures ($N_0 = 0$). We compare those finite-N_m results with expressions derived by first-order perturbation theory from the infinite-N_m eigenfunctions and find significant discrepancies. In Section III we indicate how finite coupling apertures ($N_0 \neq 0$) modify these results and derive simple mathematical expressions which approximate the machine-computed results in useful regions. In Section IV we briefly discuss the far-field

output patterns of the aperture-coupled resonator. In the final section we briefly recapitulate some of our conclusions.

II. EIGENVALUES AND EIGENFUNCTIONS WITH NO MIRROR APERTURES ($N_0 = 0$)

Using the kernal expansion-truncation technique outlined in the preceding section and in the Appendix, we have computed the eigenvalues of (9) for Fresnel numbers N_m in the range $0.6 \leqq N_m \leqq 2.0$. Where they overlap, our results agree with those of Fox and Li[1] and other authors.[10]

In our calculation we retained $M = \max(10N + 1,10)$ terms of the truncated series (13), where, if $r \geqq r_m$ is the maximum radius of interest in the field amplitudes $g_{lp}(r)$, we define $N = r_m r/\lambda b \geqq N_m$. This choice insures that the remainder

$$\left| J_l(2\pi rr') - \sum_{m=1}^{M} \frac{(-1)^{m-1}(\pi rr')^{l+2(m-1)}}{(m+l-1)!(m-1)!} \right| \tag{14}$$

will never be greater than 0.001 for the relevant radii. We have indicated in Table I for $N_m = 0.8$ and $N_0 = 0$ how the eigenvalues of the three lowest-loss modes converge as the number M of terms increases from 1 to 10.

In Fig. 2 we have plotted the power loss/pass $= 1 - |\kappa_{lp}|^2$ of the least lossy modes for $0.6 \leqq N_m \leqq 2.0$, $N_0 = 0$. It is noteworthy that no modes have less than 1 per cent loss/pass for $N_m \leqq 0.7$, that only two modes have such losses for $N_m \leqq 1.0$, but that *ten* modes have less than 1 per cent loss/pass for $N_m \leqq 2.0$. The number of low-loss modes increases very rapidly for $N_m > 1.0$ so that, whereas $N_m \leqq 1.0$ is in one sense a small Fresnel number, $N_m = 2.0$ is already rather large.

In Figs. 3–8 we have indicated for various low-order modes how the field amplitude and intensity varies with radius on the end reflecting surfaces for $N_0 = 0$ and $N_m = 0.8, 1.6$. From the intensity plots it is clear that the power loss/pass increases as the mode order increases because the higher-order eigenfunctions have more intensity lying outside the reflecting mirrors (and hence lost) than do the low-order eigenfunctions whose intensity is more concentrated near the mirror center.

From (9) and (13) it follows [compare (32) in the Appendix] that as $r \to 0$

$$g_{lp}(r) \to G_1(lp)\left[\frac{\pi^l}{l!}\right]^{\frac{1}{2}} r^l, \tag{15}$$

TABLE I

A. DEPENDENCE OF EIGENVALUES ON NUMBER M OF TERMS IN SERIES (13)*

M	κ_{00}	κ_{01}	κ_{02}
1	1.25853309	—	—
2	0.90311672	−3.6815805	—
3	1.7198455	−0.32162843	0.83714554
4	0.98489118	−1.1885874	0.24997641
5	1.0010976	−0.71086465	0.20030462
6	0.99744669	−0.77432308	0.12014589
7	0.99780308	−0.76531222	0.13087265
8	0.99777117	−0.76618958	0.12962865
9	0.99777343	−0.76612108	0.12973537
10	0.99777330	−0.76612543	0.12972805

B. CHANGE IN EIGENVALUES AS NUMBER OF TERMS IN SERIES (13) INCREASES*

M	κ_{00}	κ_{01}	κ_{02}
2-1	−0.35541637	−3.6815805	—
3-2	+0.81672878	+3.35995207	+0.83714554
4-3	−0.73495432	−0.86695897	−0.58716913
5-4	+0.01620642	+0.47772275	−0.04967179
6-5	−0.00365091	−0.06345843	−0.08015873
7-6	+0.00035639	+0.00901086	+0.0172676
8-7	−0.00003191	−0.00087736	−0.00124400
9-8	+0.00000226	+0.00006850	+0.00010672
10-9	−0.00000013	−0.00000435	−0.00000732

* Tables IA and IB are computed for the case $N_m = 0.8$, $N_0 = 0$.

where $G_1(lp)$ is a constant. This r^l dependence of the field amplitude and a corresponding r^{2l} dependence of the intensity is apparent in Figs. 3–8. Because only the angular-independent ($l = 0$) modes have nonzero intensity at $r = 0$, we anticipate that the $l = 0$ modes are much more sensitive to a coupling aperture centered at $r = 0$ than are the $l \neq 0$ modes, a fact confirmed by the finite-N_0 calculations to be discussed in the following section.

For infinite mirrors without apertures ($N_m \to \infty$, $N_0 = 0$),

$$\kappa_{lp} = (-1)^p \tag{16a}$$

and

$$g_{lp}(r) = \left[\frac{2p!}{(l+p)!}\right]^{\frac{1}{2}} (2\pi r^2)^{l/2} e^{-\pi r^2} L_p{}^l(2\pi r^2), \tag{16b}$$

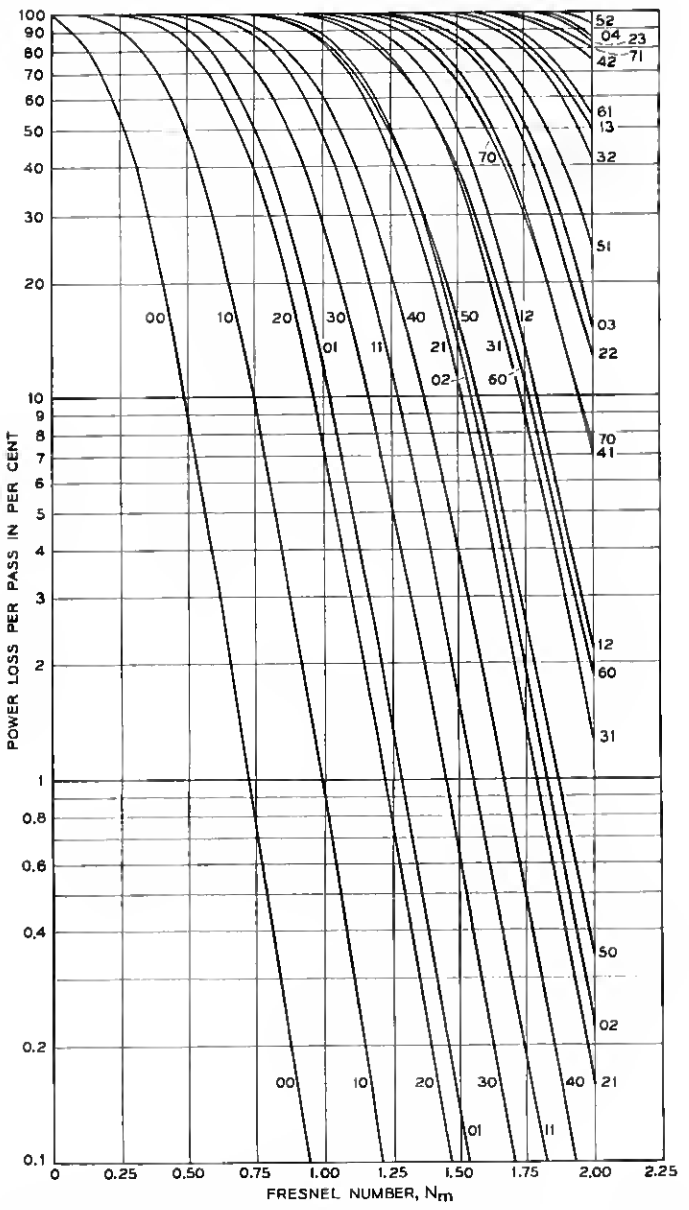

Fig. 2 — Power loss/pass versus mirror Fresnel number N_m for low-loss modes of resonator having no output-coupling aperture ($N_0 = 0$).

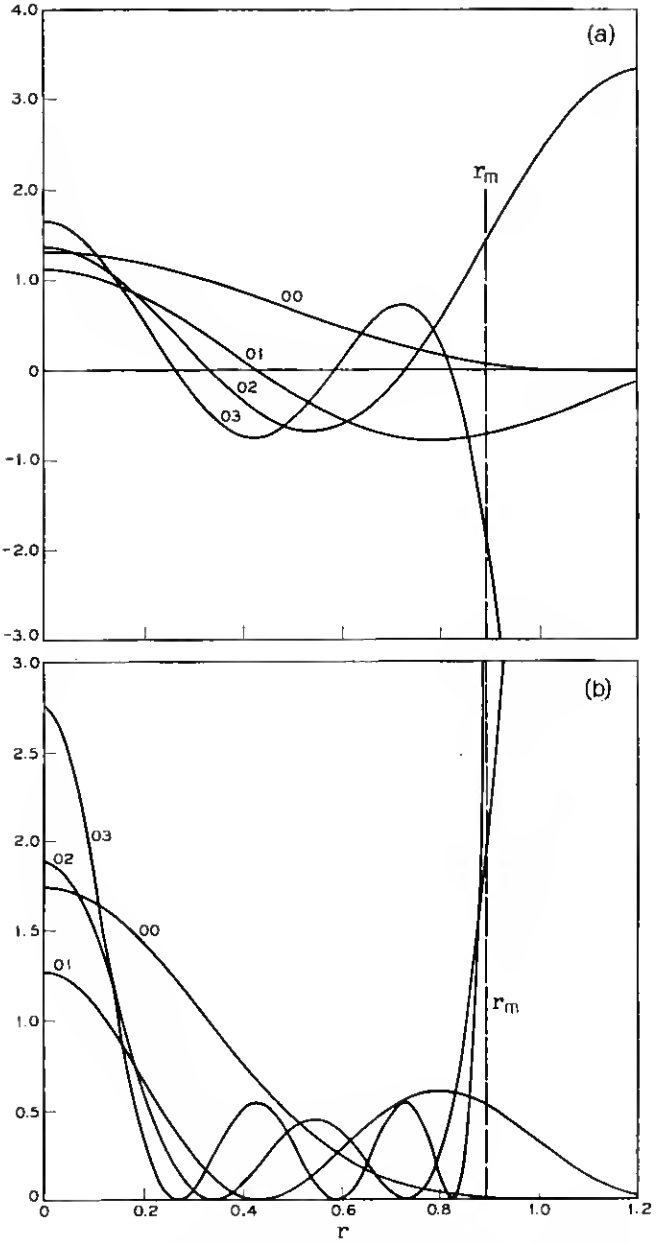

Fig. 3 — (a) Field amplitude $g_{lp}(r)$ and (b) field intensity $g_{lp}^2(r)$ for modes $(lp) = (00)$, (01), (02), and (03) with $N_m = 0.8$ and $N_0 = 0$.

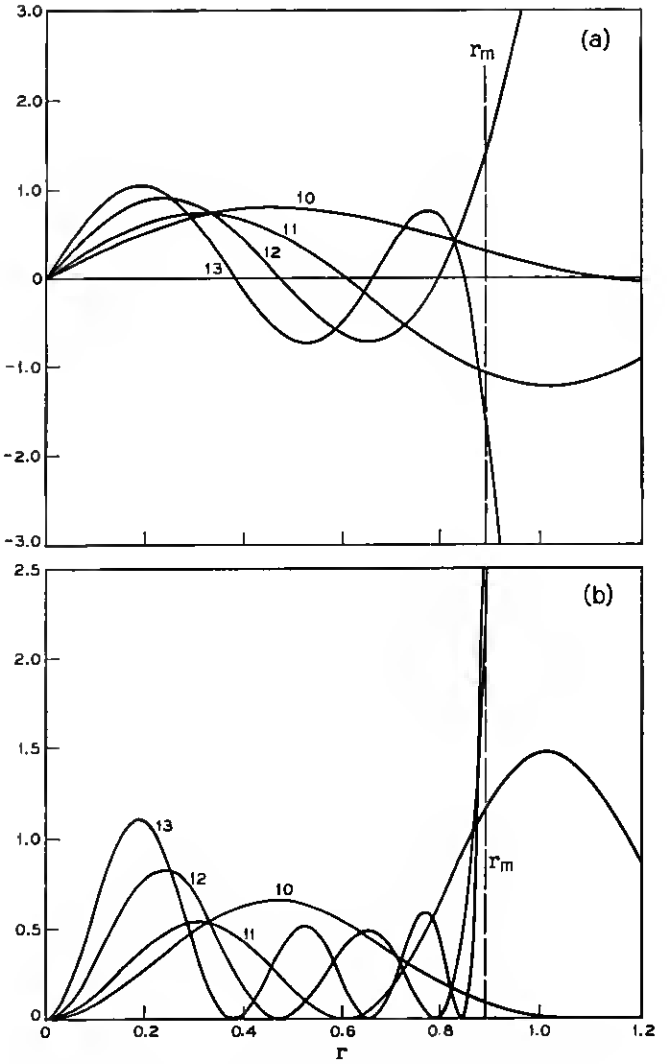

Fig. 4 — (a) Field amplitude $g_{lp}(r)$ and (b) field intensity $g_{lp}^2(r)$ for modes $(lp) = (10)$, (11), (12), and (13) with $N_m = 0.8$ and $N_0 = 0$.

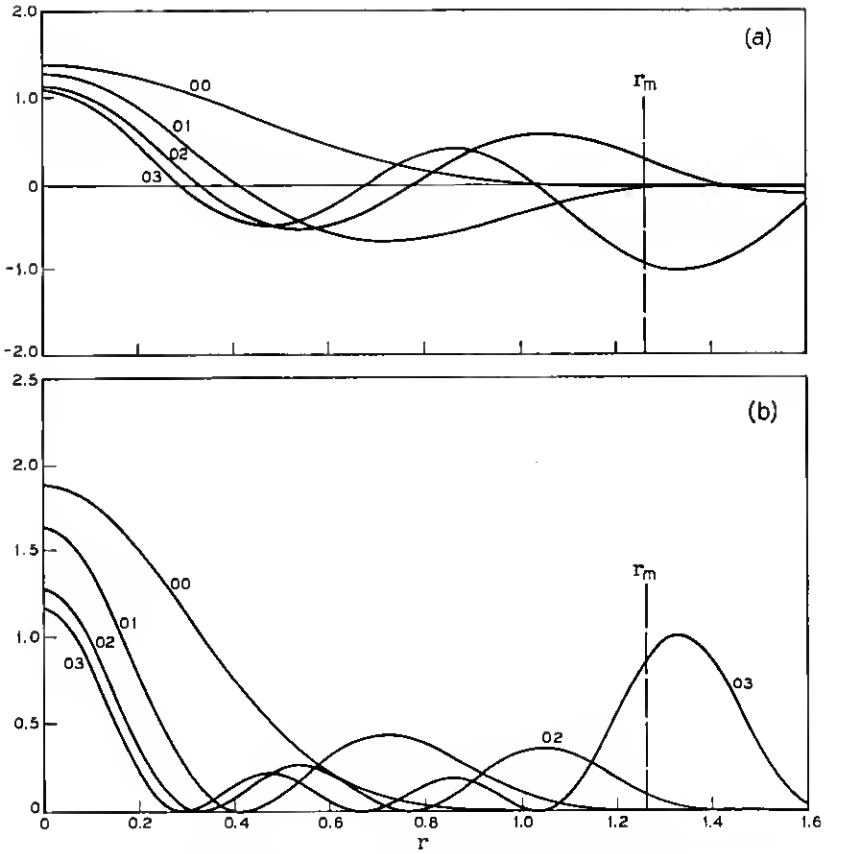

Fig. 5 — (a) Field amplitude $g_{lp}(r)$ and (b) field intensity $g_{lp}^2(r)$ for modes $(lp) = (00)$, (01), (02), and (03) with $N_m = 1.6$ and $N_0 = 0$.

where $L_p^{\,l}(z)$ is the associated Laguerre polynomial[11]

$$L_p^{\,l}(z) = \frac{e^z z^{-l}}{p!}\frac{d^p}{dz^p}(e^{-z}z^{p+l}) = \sum_{m=0}^{p}\frac{(p+l)!(-z)^m}{(p-m)!(l+m)!m!}. \quad (17)$$

Low-order Laguerre polynomials are

$$L_0^{\,l}(z) = 1; \qquad L_1^{\,l}(z) = l + 1 - z;$$

$$L_2^{\,l}(z) = \tfrac{1}{2}[(l+2)(l+1) - 2z(l+2) + z^2].$$

The finite-N_m results we have computed transform continuously into the solutions (16) as N_m increases. If for $N_0 = 0$ and arbitrary N_m the

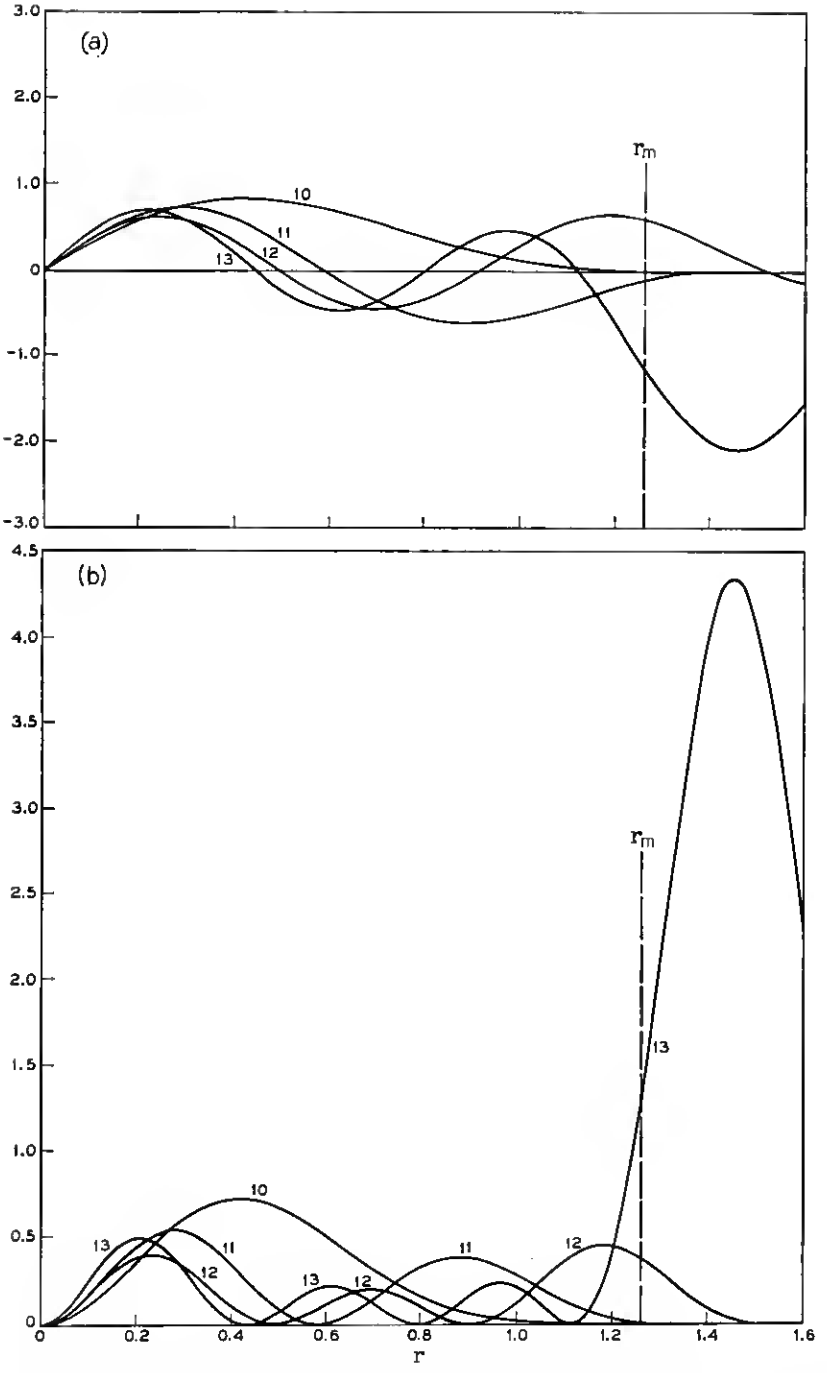

Fig. 6 — (a) Field amplitude $g_{lp}(r)$ and (b) field intensity $g_{lp}^2(r)$ for modes $(lp) = (10)$, (11), (12), and (13) with $N_m = 1.6$ and $N_0 = 0$.

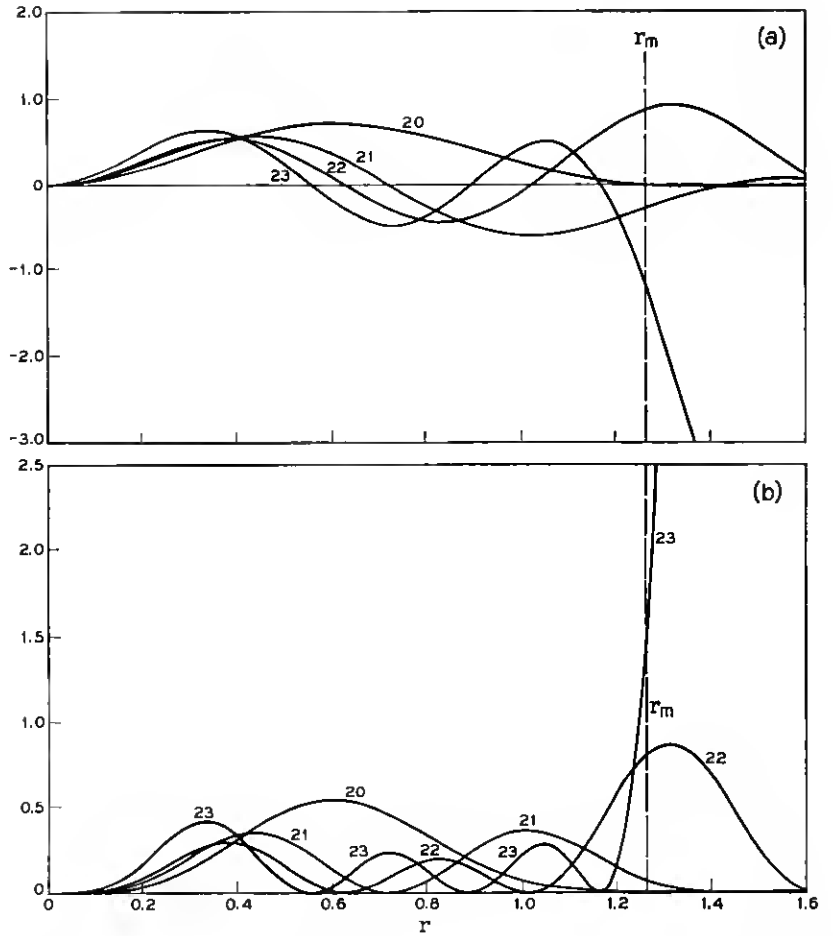

Fig. 7 — (a) Field amplitude $g_{lp}(r)$ and (b) field intensity $g_{lp}^2(r)$ for modes $(lp) = (20)$, (21), (22), and (23) with $N_m = 1.6$ and $N_0 = 0$.

integer $p \geqq 0$ orders the eigenmodes of a given angular quantum number l with respect to increasing power loss/pass, then the eigenvalue

$$\kappa_{lp} = (-1)^p \, | \, \kappa_{lp} \, | \tag{18}$$

and the amplitude function has p zeros in the interval $0 < r < r_m$.

If we assume for finite N_m that the low-loss eigenfunctions approximate the limiting expressions (16b), we can estimate the deviation of κ_{lp} from its infinite-N_m value (16a) by first-order perturbation theory:

$$1 - (-1)^p \kappa_{lp} \text{ (pert)} = \int_{2\pi N_m}^{\infty} dx \, x^l e^{-x} [L_p^{\,l}(x)]^2. \tag{19}$$

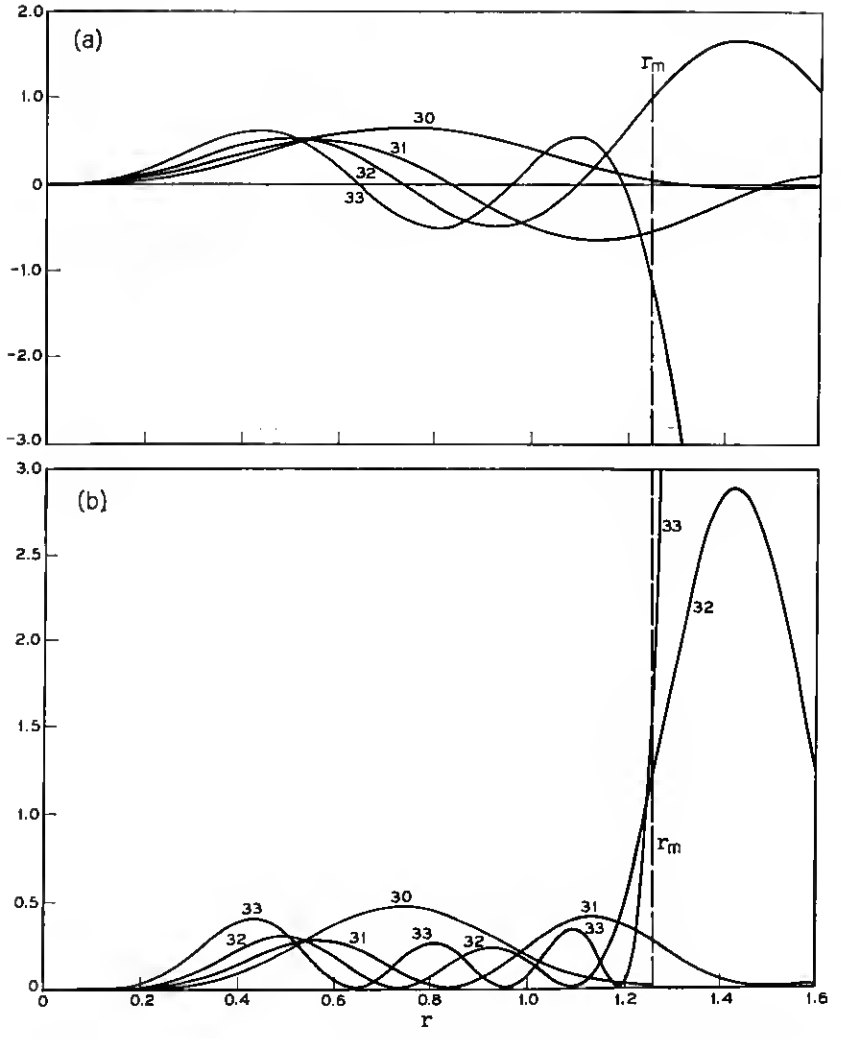

Fig. 8 — (a) Field amplitude $g_{lp}(r)$ and (b) field intensity $g_{lp}^2(r)$ for modes $(lp) = (30)$, (31), (32), and (33) with $N_m = 1.6$ and $N_0 = 0$.

Two special cases are

$$1 - \kappa_{00} \text{ (pert)} = e^{-2\pi N_m}, \qquad 1 + \kappa_{01} \text{ (pert)} = [1 + (2\pi N_m)^2]e^{-2\pi N_m}.$$

We compare these estimates with computed values in Table II. The errors between the computed and estimated values in Table II, while small relative to the eigenvalues themselves, are nevertheless significant

TABLE II — DEVIATION OF EIGENVALUES FROM INFINITE-MIRROR VALUES (16b)

N_m*	$1 - \kappa_{00}$	$1 - \kappa_{00}$(pert)†	$1 - \kappa_{00}$(asym)††	$1 + \kappa_{01}$	$1 + \kappa_{01}$(pert)†	$1 + \kappa_{01}$(asym)††
0.6	1.82×10^{-2}	2.31×10^{-2}	2.52×10^{-2}	0.545	0.351	5.73
0.8	2.23×10^{-3}	6.56×10^{-3}	2.72×10^{-3}	0.234	0.172	1.099
1.0	2.38×10^{-4}	1.87×10^{-3}	2.75×10^{-4}	6.37×10^{-2}	7.56×10^{-2}	0.174
1.2	2.38×10^{-5}	5.31×10^{-4}	2.68×10^{-5}	1.20×10^{-2}	3.07×10^{-2}	2.43×10^{-2}
1.4	2.24×10^{-6}	1.51×10^{-4}	2.53×10^{-6}	1.80×10^{-3}	1.19×10^{-2}	3.13×10^{-3}
1.6	$\sim 2.7 \times 10^{-7}$ ‡	4.31×10^{-5}	2.34×10^{-7}	2.40×10^{-4}	4.39×10^{-3}	3.79×10^{-4}

* $N_0 = 0$.
† Estimated values computed from (19) of first-order perturbation theory.
†† Estimated values computed from asymptotic (20).
‡ The accuracy of κ_{00} for $N_m = 1.6$ is limited by machine rounding errors.

when compared to the difference $1 - (-1)^p \kappa_{lp} = 1 - |\kappa_{lp}|$ which for these eigenvalues is roughly one-half the power loss/pass (13). The errors arise because the real eigenfunctions are not identical to the limiting expressions (16a). Slepian[5] has derived more accurate asymptotic results appropriate to N_m large:

$$1 - (-1)^p \kappa_{lp}(\text{asym}) = \frac{\pi (8\pi N_m)^{l+2p+1} e^{-4\pi N_m}}{p!(l+p)!} \left[1 + 0\left(\frac{1}{N_m}\right)\right]. \quad (20)$$

Two special cases are

$$1 - \kappa_{00}\ (\text{asym}) = 8\pi^2 N_m e^{-4\pi N_m}; \qquad 1 + \kappa_{01}(\text{asym}) = \pi (8\pi N_m)^3 e^{-4\pi N_m}.$$

Values computed from these expressions are also listed in Table II.

In Table III we have listed values at $r = 0$ of $g_{lp}(r)$ for $(lp) = (00)$, (01), and (02). These values are consistently less than the values predicted from the infinite-N_m functions (16b) renormalized to the finite interval $(0, r_m)$:

$$g_{lp}(r) = \left[\frac{2p!}{(l+p)!}\right]^{\frac{1}{2}} (2\pi r^2)^{l/2} e^{-\pi r^2} L_p^{\,l}(2\pi r^2) \times \left\{1 - \frac{p!}{(l+p)!} \int_{2\pi N_m}^{\infty} dx\, x^l\, e^{-x} [L_p^{\,l}(x)]^2\right\}^{-\frac{1}{2}} \quad (21)$$

for which

$$g_{0p}(0) = 2^{\frac{1}{2}} \left\{1 - \int_{2\pi N_m}^{\infty} dx\, e^{-x} [L_p^{\,0}(x)]^2\right\}^{-\frac{1}{2}}. \quad (22)$$

The differences between the calculated and estimated results again reflect the distortion appropriate to finite N_m of the eigenfunctions (16b).[5] For a given angular quantum number l, this distortion is generally less

TABLE III — FIELD AMPLITUDE AT MIRROR CENTER FOR $l = 0$ MODES

N_m*	$g_{00}(0)$	$g_{01}(0)$	$g_{02}(0)$
0.6	1.277	1.225	1.616
0.8	1.321	1.125	1.373
1.0	1.346	1.151	1.193
1.2	1.360	1.209	1.089
1.4	1.369	1.253	1.081
1.6	1.375	1.281	1.130
2.0	1.384	1.315	1.220
∞	$\sqrt{2} = 1.414$	1.414	1.414

* $N_0 = 0$.

significant in low-order modes than it is in high-order modes. (The former are usually the only modes relevant to laser oscillators.) That this is so can be understood if we recall that for the cylindrical confocal geometry $g_{lp}(r)$ will have p zeros in the interval $r_0 < r < r_m$. As the interval (r_0, r_m) is compressed within the interval $(0, \infty)$ appropriate to (16a,b), those functions $g_{lp}(r)$ whose zeros initially lay outside (r_0, r_m) will clearly be more distorted by the compression than will those functions which have no zeros $(p = 0)$ or those whose zeros lie well within (r_0, r_m). In Table IV we have tabulated the zeros within (r_0, r_m) of several low-loss eigenfunctions for different N_m.

III. EIGENMODES FOR FINITE MIRROR APERTURES $(N_0 \neq 0)$

In this section, in order to distinguish the $N_0 = 0$ and the $N_0 \neq 0$ results, we mark the eigenvalues and eigenfunctions for $N_0 = 0$ by a superscript "0": $\kappa_{lp}^{0}, g_{lp}(r)^{0}$. As in the preceding section, we assign the integer $p \geqq 0$ to the $N_0 = 0$ modes in the order of their increasing power loss/pass: $|\kappa_{lp}^{0}| > |\kappa_{lp+1}^{0}|$. We identify the $N_0 \neq 0$ modes by

TABLE IV — ZEROS OF $g_{lp}(r)$ IN THE DOMAIN $0 = r_0 < r < r_m$

N_m*	r_m‡	$l = 0$	0		1	1		2	2	
		p† = 1	2_1	2_2	1	2_1	2_2	1	2_1	2_2
0.6	0.775	0.434	0.318	0.662	0.573	0.432	0.699	0.641	0.502	0.718
0.8	0.894	0.433	0.339	0.735	0.604	0.474	0.792	0.705	0.560	0.821
1.0	1.000	0.425	0.345	0.772	0.606	0.496	0.859	0.734	0.599	0.903
1.2	1.095	0.418	0.342	0.780	0.598	0.504	0.897	0.737	0.621	0.965
1.4	1.183	0.414	0.336	0.774	0.590	0.501	0.909	0.729	0.628	1.002
1.6	1.265	0.412	0.330	0.766	0.585	0.493	0.905	0.721	0.626	1.016
∞	∞	0.399	0.305	0.707	0.564	0.449	0.868	0.691	0.564	0.977

* $N_0 = 0$.
† The function $g_{lp}(r)$ has p zeroes in $r_0 < r < r_m$.
‡ $r_m = N_m$‡.

the indices that those modes would carry if they deformed continuously from $N_0 = 0$. As we shall see, it is uot necessary that $|\kappa_{lp}| > |\kappa_{lp+1}|$ when $N_0 \neq 0$; however, the $N_0 \neq 0$ modes do have the properties (15) and (18) of the $N_0 = 0$ modes. In additiou, the field amplitude $g_{lp}(r)$ will continue to have p zeros in the reflecting interval $r_0 < r < r_m$ ($r_0 = 0$ for $N_0 = 0$).

Using perturbation theory to express the $N_0 \neq 0$ eigenfunctions in terms of the $N_0 = 0$ functions, we have to first order:[12]

$$g_{lp}(r) = g_{lp}(r)^0 \left\{1 + \pi \int_0^{r_0} dr'\, r'[g_{lp}(r')^0]^2\right\} - \sum_{q\neq p}{}' \frac{g_{lq}(r)^0}{\kappa_{lp}{}^0 - \kappa_{lq}{}^0} \kappa_{lq}{}^0 2\pi \int_0^{r_0} dr'\, r' g_{lp}(r')^0 g_{lq}(r')^0. \tag{23}$$

To second order, the eigenvalues are

$$\kappa_{lp} = \kappa_{lp}{}^0 \left\{1 - 2\pi \int_0^{r_0} dr\, r[g_{lp}(r)^0]^2\right\} + \sum_{q\neq p}{}' \frac{\kappa_{lp}{}^0 \kappa_{lq}{}^0}{\kappa_{lp}{}^0 - \kappa_{lq}{}^0} \left[2\pi \int_0^{r_0} dr\, r g_{lp}(r)^0 g_{lq}(r)^0\right]^2. \tag{24}$$

The factor multiplying $g_{lp}(r)^0$ in (23) is a normalization correction compensating for the fact that the $g_{lp}(r)$ are normalized in (10) over the interval (r_0, r_m), whereas the $g_{lp}(r)^0$ are normalized over the larger interval $(0, r_m)$. The first-order correction to the eigenvalue in the first term of (24) decreases the unperturbed eigenvalue $\kappa_{lp}{}^0$ by that fraction of the unperturbed field intensity which falls on the aperture.

The second terms in (23) and (24) describe eigenfunction mixing by the aperture. The amount of mixing depends upon the eigenvalue difference as well as upon the strength of the perturbative coupling. The circular apertures, centered on the resonator axis, do not mix modes with different angular quantum numbers. Because the signs of the eigenvalues alternate as in (18), mode mixing in the symmetric identical-mirror cavity is strongest among modes with the same p parity $(-1)^p$. The situation is somewhat different in resonators with dissimilar mirrors such as obtains in the apparatus of Patel et al.[2] where only one mirror is pierced by the output-coupling aperture. In such systems there is significant mixing between even-p and odd-p modes.[4]

Whereas mode mixing will preclude two eigenvalues from actually crossing (if the two modes are coupled by the perturbation), there is, because of the sign property (18), no such restriction on the absolute values $|\kappa_{lp}|$ and $|\kappa_{lp+1}|$ or, equivalently, on the diffraction losses of the (lp) and $(lp + 1)$ modes. For some special values of (N_0, N_m) one can

in fact reverse the power-loss progression of the $N_0 = 0$ case to give $|\kappa_{lp+1}| > |\kappa_{lp}|$; however, it is always true for the identical-mirror cylindrical confocal system that

$$|\kappa_{lp}| > |\kappa_{lp+2}| . \tag{25}$$

In more general geometries with more complicated eigenvalue phase relations than (18) even this restricted condition can be violated.

Using the kernel expansion-truncation method outlined in the Appendix, we have computed the effects of finite coupling apertures on the properties of cavity eigenmodes. In Fig. 9 we have indicated for a Fresnel number $N_m = 0.8$ how a finite coupling aperture with Fresnel number $N_0 \neq 0$ affects the loss/pass of the lowest-order modes. In the confocal geometry the finite aperture affects only the magnitude of the eigenvalues; their signs (phases) are still given by (18). In no case do the eigenvalues belonging to the same angular quantum number l cross

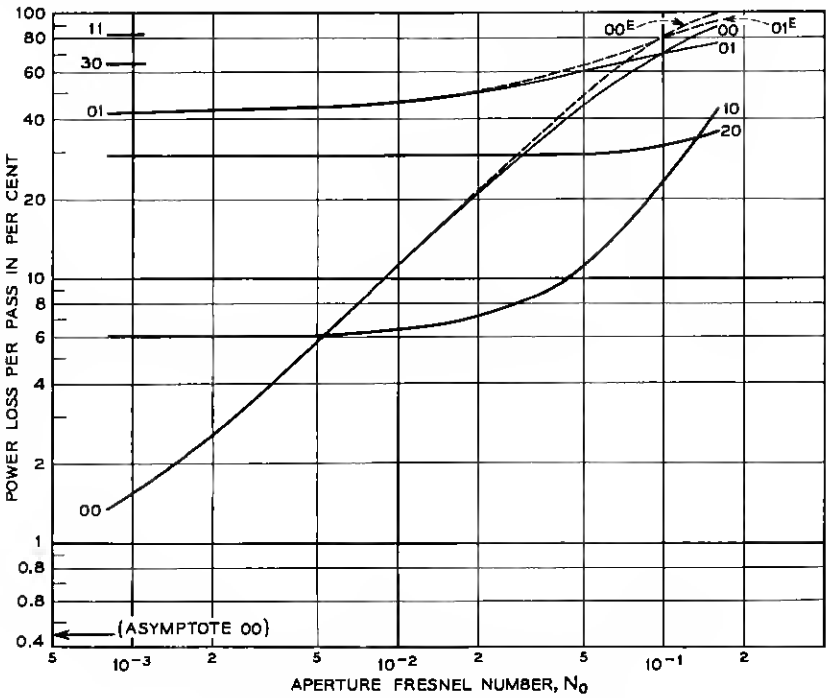

Fig. 9 — Power loss/pass versus aperture Fresnel number N_0 for low-loss modes with $N_m = 0.8$. Dashed curves (00^E) and (01^E) are estimates based on (26b).

(the circular-aperture perturbations do not couple modes with different l), although in Fig. 9 we do see for the (00) and (01) modes a reversal of the $N_0 = 0$ sequence $|\kappa_{00}| > |\kappa_{01}|$ in the interval $0.08 < N_0 < 0.16$.

Fig. 9 confirms our previous conjecture that the modes with angular quantum number $l = 0$ are more sensitive to deleterious aperture loss than are the $l \neq 0$ modes. When for $N_m = 0.8$ the area of the aperture is only 0.6 per cent of the total mirror area ($N_0/N_m = 0.006$), the loss/pass of the (00) mode has increased to the point where it equals the loss/pass of the (10) mode. For this same hole size the losses of the (10) mode are virtually uuaffected by the aperture.

In Fig. 10 we have indicated the intensity distribution of the (00) mode for $N_m = 0.8$ and $N_0 = 0, 0.01$. Except for the normalization correction implicit in the first term of (23), the intensity distribution for $N_0 = 0.01$ is nearly identical to that for $N_0 = 0$. We conclude for $N_m = 0.8$ and $N_0 \lesssim 0.01$ that eigenfunction mixing in (23) is unimportant and, as a consequence, that the eigenvalues are accurately given by the first-order term of (24). Using the infinite-N_m functions (16b) to approximate $g_{lp}(r)^0$ in the first term of (24), we can estimate the ratio $\kappa_{lp}/\kappa_{lp}^0$ analytically. For $l = 0$ this estimate can be considerably improved if we renormalize the infinite-N_m functions (16b) by the factor $g_{0p}(0)/\sqrt{2}$ computed from Table III. Doing this, we estimate

$$\kappa_{0p} = \kappa_{0p}^0 \left\{ 1 - \frac{1}{2} [g_{0p}(0)^0]^2 \int_0^{2\pi N_0} dx\, e^{-x} [L_p^0(x)]^2 \right\}. \qquad (26a)$$

where κ_{lp}^0 and $g_{lp}(0)^0$ are implicitly dependent upon N_m. In the limit

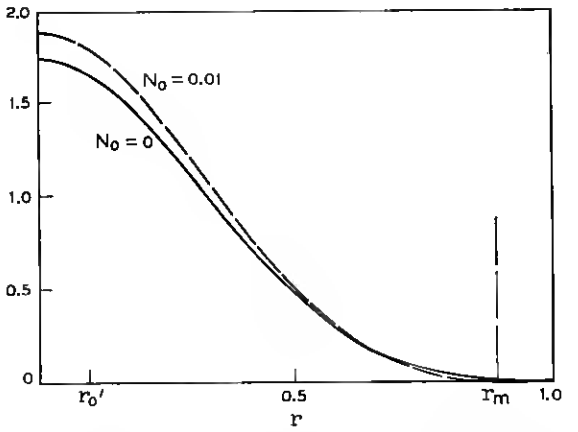

Fig. 10 — Field intensity $g_{lp}^2(r)$ of the mode $(lp) = (00)$ for $N_m = 0.8$ with $N_0 = 0$ (solid curve) and $N_0 = 0.01$ (dashed curve). ($N_m \equiv r_m^2$; $N_0 \equiv r_0^2$.)

of small N_0, for whicb we can in effect replace $g_{lp}(r)^0$ by $g_{lp}(0)^0$ in tbe rigbt-hand side of (24), this gives

$$\kappa_{0p} = \kappa_{0p}{}^0\{1 - \pi N_0[g_{0p}(0)^0]^2\}. \quad (26b)$$

To the same accuracy, the r^l dependence of $g_{lp}(r)$ noted in (15) implies tbat $\kappa_{lp} = \kappa_{lp}{}^0$ for $l \neq 0$. Tbe approximation (26b) has been used to compute the dasbed curves in Fig. 9. For $N_0 \lesssim 0.02$ the fit to the machine-computed curves is excellent.

Tbe effect of a finite aperture ($N_0 \neq 0$) on the losses of the low-loss modes for $N_m = 1.6$ is indicated in Fig. 11. More modes are sbown than

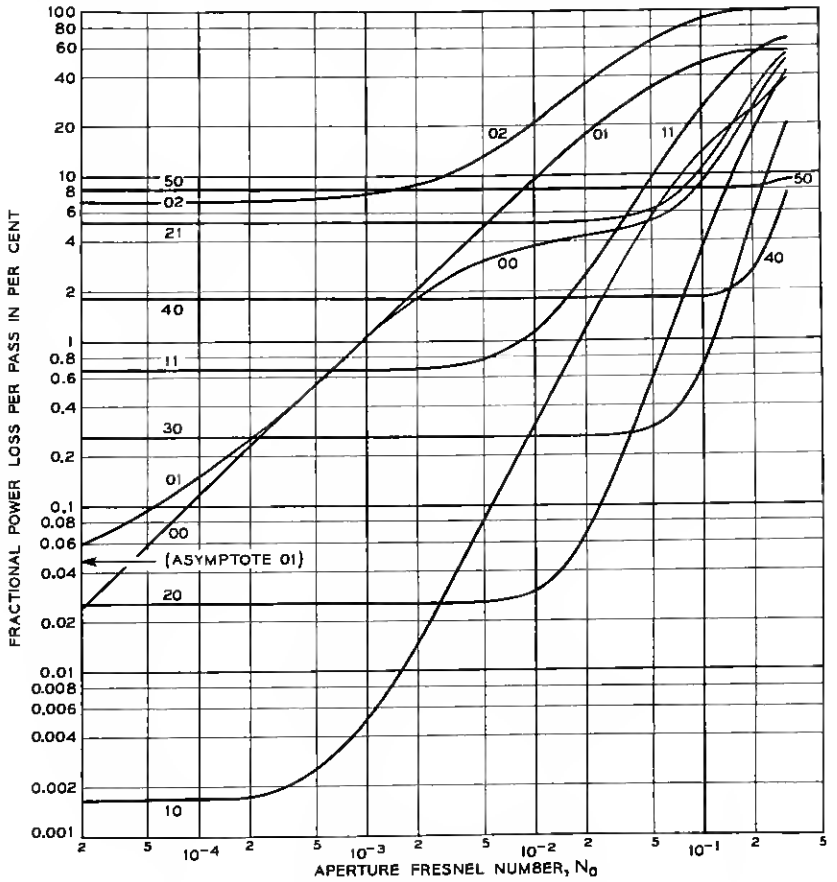

Fig. 11 — Power loss/pass versus aperture Fresnel number N_0 for low-loss modes with $N_m = 1.6$.

in Fig. 9 because at the larger Fresnel number more modes have low loss (cf. Fig. 2). Observe for any fixed radial quantum number p that, consistent with the r^l behavior noted in (15), modes with low angular quantum number l are more sensitive to a small aperture than are the modes with higher angular quantum number. The sequence in Fig. 11 of upward breaks in the losses of the modes (00), (10), (20), $\cdots$ is particularly striking, as is that for the modes (01), (11), (21), $\cdots$.

In Fig. 12 we have redrawn those curves of Fig. 11 which pertain to the angular-invariant $l = 0$ modes. The dashed curves in Fig. 12 derive from the approximation (26b), which is here valid only for $N_0 \lesssim 0.0005$ in the (00) and (02) modes and for $N_0 \lesssim 0.006$ in the (01) mode. [For $N_m = 0.8$ it applied to all $N_0 \lesssim 0.02$.] The approximation (26b), based upon first-order perturbation theory, fails when eigenfunction mixing becomes significant. Mixing is strong for the (00) mode when the losses of that mode due to the finite aperture approximate the edge

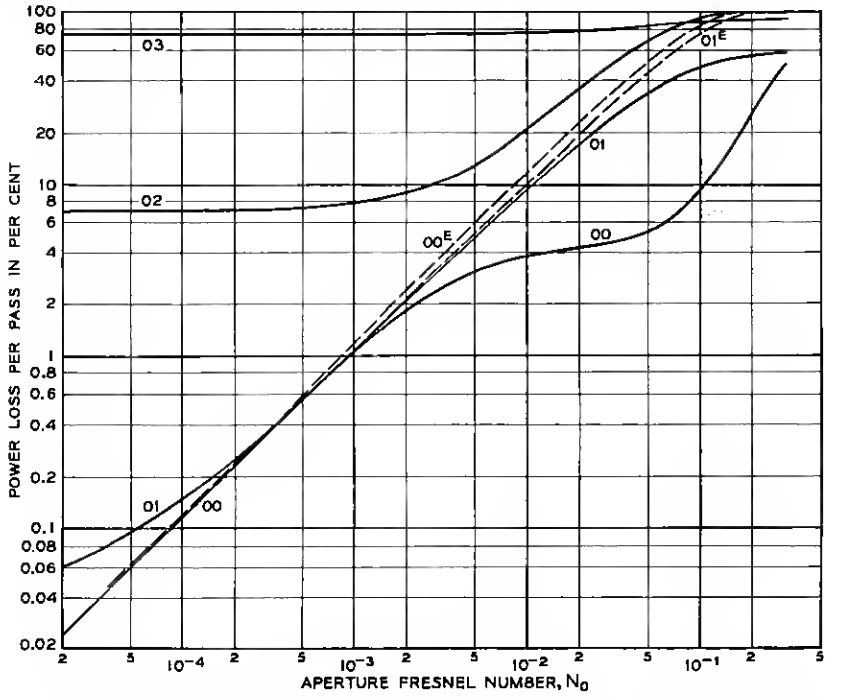

Fig. 12 — Power loss/pass versus aperture Fresnel number N_0 for the low-loss $l = 0$ modes with $N_m = 1.6$. Dashed curves (00^E) and (01^E) are estimates based on (26b).

losses of the (02) mode — that is, when $\kappa_{00} \approx \kappa_{02}$. If we recall that a variational principle applies to the present eigenvalue problem [because, in contradistinction to more general resonator kernels, the kernel in the integral equation (9) is Hermitian], we can view mode mixing as an attempt by the field in the low-loss (00) mode to reduce its intensity at the aperture and to reduce thereby the total (00) loss. Because edge as well as aperture losses contribute to the total loss, the deleterious edge losses of the (02) mode preclude appreciable (00)-(02) mixing until the aperture losses of the undistorted (00) mode approximate the edge losses of the (02) mode. Because edge losses decrease rapidly with increasing N_m ($N_m = 1.6$ is already quite large), the aperture losses required for appreciable mixing decrease rapidly with increasing N_m. The relevance of mode mixing to the breakdown of (26b) is clearly illustrated in Fig. 13, where we show the intensity distribution of the (00) mode for $N_m = 1.6$ and $N_0 = 0$, 0.01, and 0.02. [The same aperture Fresnel numbers N_0 gave insignificant mode distortion for $N_m = 0.8$ (Fig. 10).]

In Fig. 14 is shown the intensity distribution for three other low-order $l = 0$ modes besides the (00) mode for $N_m = 1.6$ and $N_0 = 0.01$. This figure should be compared with Fig. 5b, which shows the intensity distribution of the same modes for $N_m = 1.6$ and $N_0 = 0$. Note that, whereas the intensity at $r = 0$ of the (00) mode decreased as a result of aperture mode mixing, the intensity at $r = 0$ of the (02) mode increased. This increase is reflected in Fig. 12 in the sharp rise of (02) losses as the (00) and (02) eigenvalues "repel" for $N_0 \gtrsim 0.003$.

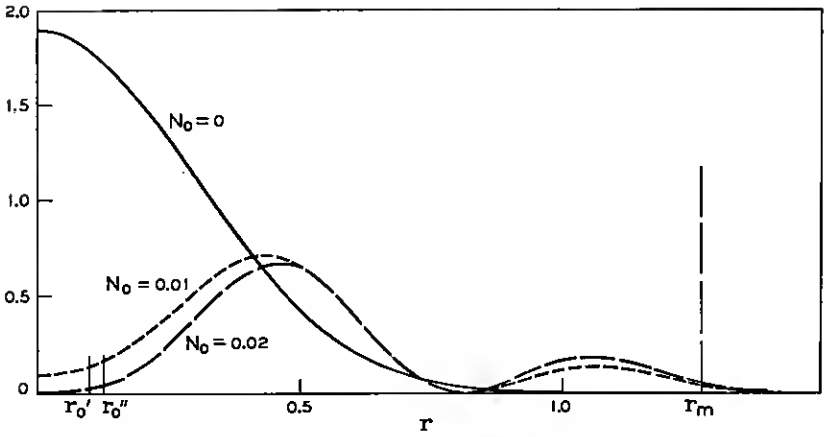

Fig. 13 — Field intensity $g_{lp}^2(r)$ of the mode $(lp) = (00)$ for $N_m = 1.6$ with $N_0 = 0$ (solid curve) and $N_0 = 0.01$, 0.02 (dashed curves). ($N_m \equiv r_m^2$; $N_0 \equiv r_0^2$.)

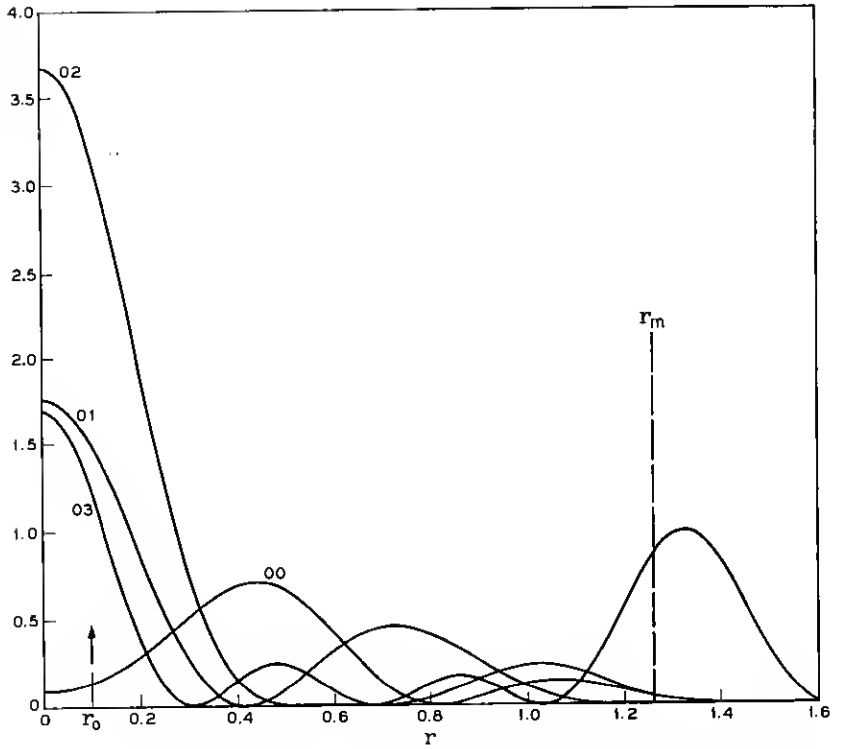

Fig. 14 — Field intensity $g_{1p}^2(r)$ of the low-loss $l = 0$ modes for $N_m = 1.6$ and $N_0 = 0.01$. ($N_m \equiv r_m^2$; $N_0 \equiv r_0^2$.) Notice how mode mixing has changed the intensity distribution near the aperture ($0 \leqq r < r_0$) from that in Fig. 5(b) where $N_0 = 0$.

In Figs. 15, 16, and 17 we have indicated how the power loss/pass of the low-loss modes varies when for fixed aperture size N_0 the Fresnel number N_m changes. Notice in the typical Fig. 15 that the losses of the (00) mode decrease as N_m increases from N_0 until for $N_m \approx 0.7$ those losses saturate at about 11 per cent/pass, approximately the loss predicted from (26b) with $g_{00}(0)^0 = \sqrt{2}$ and $\kappa_{00}{}^0 = 1$. As N_m increases beyond 1.3, mode mixing reduces the losses of the (00) mode as the modified intensity distribution avoids both the aperture and the reflector edges. While by $N_m = 1.6$ the (00) mode again has the lowest loss of the $l = 0$ modes, its total loss is greater than that of certain $l \neq 0$ modes and its intensity distribution (Fig. 13) is considerably different from the simple Gaussiau of (16b).

A quantity of interest in the design of lasers with aperture output

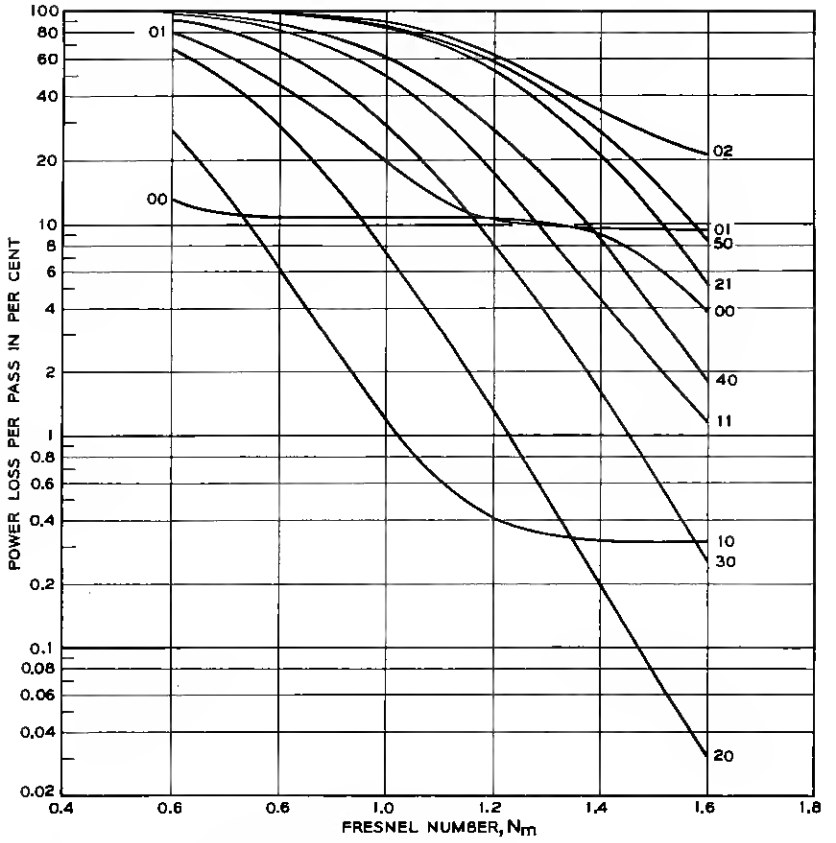

Fig. 15 — Power loss/pass of low-loss modes versus Fresnel number N_m for aperture Fresnel number $N_0 = 0.01$.

coupling[2] is that value N_{0c} of N_0 for which the losses of the (00) mode equal the losses of the (10) mode. All other things being equal, the laser will oscillate in the (00) mode for $N_0 < N_{0c}$, whereas for $N_0 > N_{0c}$ it will operate in the (10) mode or, for large values of N_0, in still another mode (cf. Fig. 11). In Fig. 18 we have plotted N_{0c} as a function of N_m. For $N_m > 0.6$ this curve can be accurately reproduced by the following expression based upon (26b):

$$N_{0c} = (\kappa_{00}^{0} - \kappa_{10}^{0})/\pi\kappa_{00}^{0}[g_{00}(0)^{0}]^2. \tag{27}$$

This result obtains even for large N_m because N_{0c} decreases so rapidly with increasing N_m that mode mixing is never relevant.

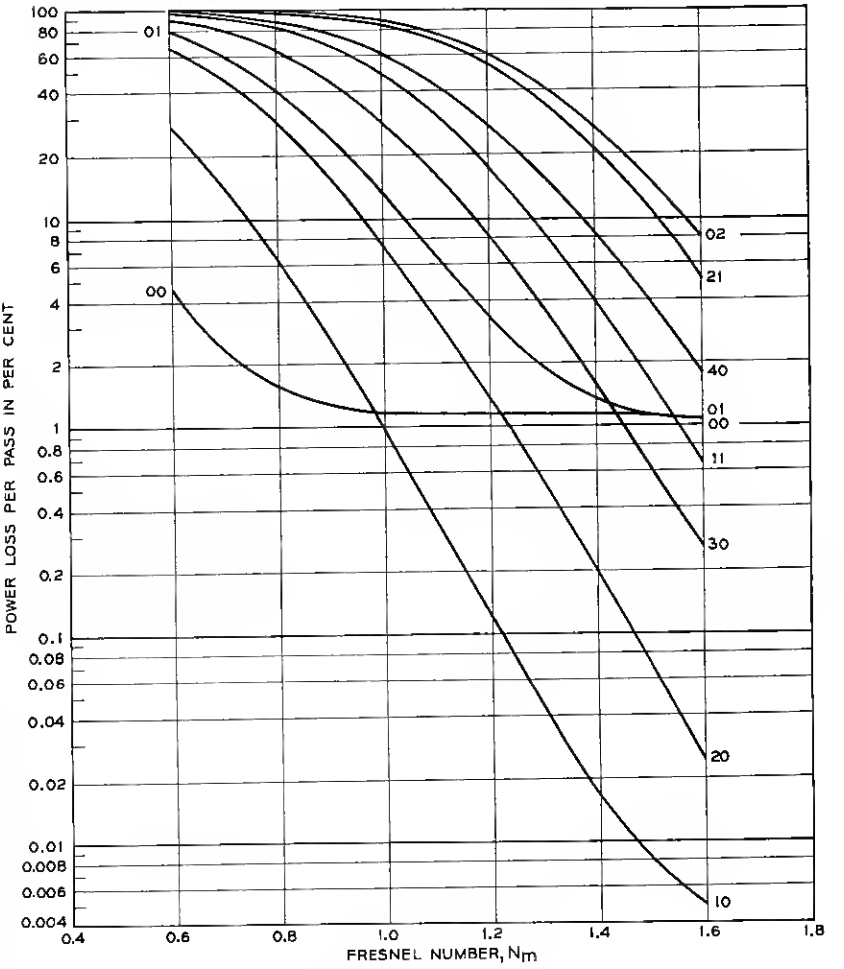

Fig. 16 — Power loss/pass of low-loss modes versus Fresnel number N_m for aperture Fresnel number $N_0 = 0.001$.

IV. FAR-FIELD PATTERNS, APERTURE OUTPUT COUPLING

If we assume that the useful output coupling of the mode (lp) is exclusively through one of the small reflector apertures of Fresnel number N_0, then at a large distance d from the relevant output aperture and in a direction making an angle θ with the cavity axis (see Fig. 19) the field amplitude will be proportional to

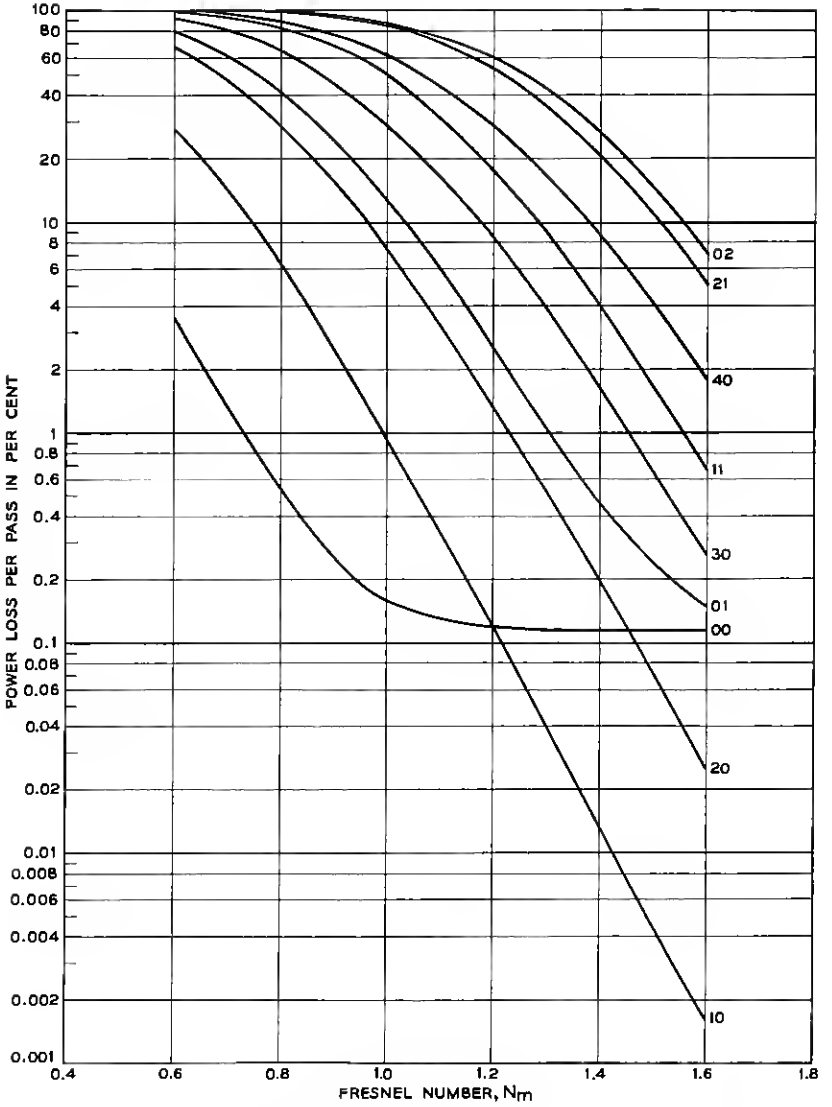

Fig. 17 — Power loss/pass of low-loss modes versus Fresnel number N_m for aperture Fresnel number $N_0 = 0.0001$.

$$A_{lp}(\theta,\varphi) = e^{-il\varphi}\frac{2\pi b}{d}\int_0^{r_0} dr\, rJ_l[2\pi r(b/\lambda)^{\frac{1}{2}}\sin\theta]g_{lp}(r). \qquad (28)$$

Here φ is the azimuthal angle used in (1); r is the radial variable defined in (6); and $g_{lp}(r)$ is the mirror-field amplitude function (8). The derivation of (28) from the Fraunhofer formula parallels that of (2) and (9).[1] The basic approximation used is

$$[d^2 + \rho^2 - 2\rho d\sin\theta\cos\varphi\,]^{\frac{1}{2}} \approx d - \rho\sin\theta\cos\varphi. \qquad (29)$$

This approximation is suitable when $d \gg a_0 \geqq \rho$ and $a_0^2/\lambda d = bN_0/d \ll 2$.

In the important case for which r_0 is so small ($N_0 \lesssim N_{0c}$ is sufficient)

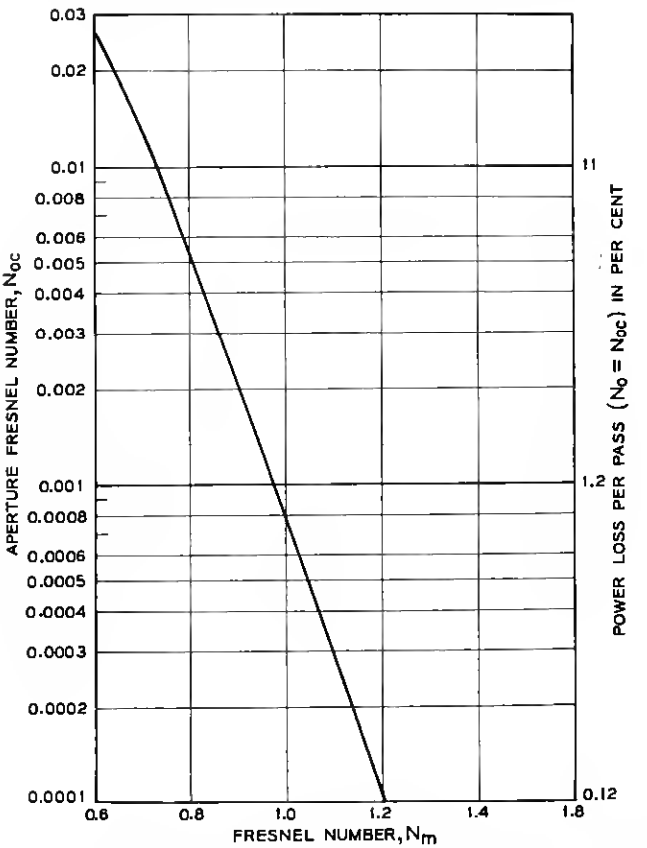

Fig. 18 — Critical aperture Fresnel number N_{0c} for which diffraction losses of (00) mode equal those of (10) mode versus Fresnel number N_m. Also shown for each Fresnel number N_m is the loss/pass when $N_0 = N_{0c}$. This loss is approximately, but not exactly, proportional to N_{0c}.

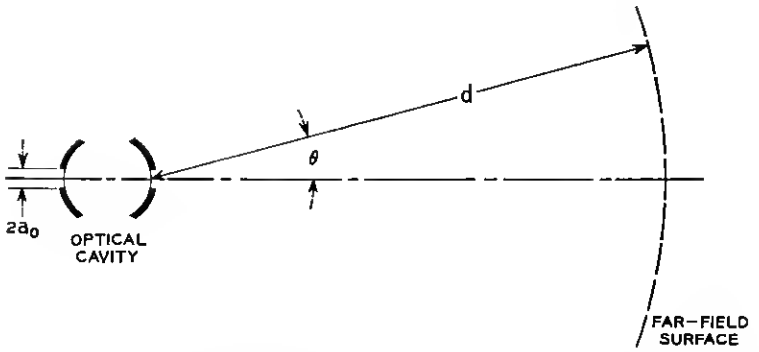

Fig. 19 — Geometry appropriate to the analysis of the far-field pattern for aperture output coupling of cavity.

that we can approximate $g_{lp}(r)$ by the lowest-order term (15), we obtain from (28):

$$A_{lp}(\theta,\varphi) = \frac{1}{l!}\frac{d^l g_{lp}}{dr^l}\bigg|_{r=0} e^{-il\varphi}\left(\frac{a_0 N_0^{\,l/2}}{d\sin\theta}\right) J_{l+1}\left(\frac{2\pi a_0 \sin\theta}{\lambda}\right). \tag{30}$$

The observed intensity pattern for a pure l mode will be proportional to

$$I_{lp}(\theta,\varphi) = \left[\frac{1}{l!}\frac{d^l g_{lp}}{dr^l}\bigg|_{r=0}\left(\frac{a_0 N_0^{\,l/2}}{d\sin\theta}\right)\right]^2 \cos^2[l(\varphi-\delta_l)]J_{l+1}{}^2\left(\frac{2\pi a_0\sin\theta}{\lambda}\right), \tag{31}$$

where δ_l is an appropriate phase angle. For $l = 0$ this gives the celebrated Airy diffraction pattern.[13]

V. SUMMARY REMARKS

We have computed the eigenmodes of a symmetric cylindrical confocal laser cavity of Fresnel number $N_m \leqq 2.0$ and have determined how those modes change when a small circular element centered on the axis is removed from each reflector. The calculation methods can easily be adapted to cylindrical confocal resonators for which the two mirrors and mirror apertures have different sizes. (Results relevant to a coupling aperture in only one end reflector will be published in a subsequent article.) The basic expansion-truncation methods outlined in Section I and in the Appendix are quite general[10] and can usefully be applied to nonconfocal geometries for which complex-number computations are required when the mirror surfaces are not surfaces of constant phase.

For the cylindrical confocal geometry the results reported above indicate that, while the infinite-N_m functions with appropriate normalization do approximate the low-order finite-N_m eigenfunctions,

there are significant differences which influence the calculation of both aperture and edge diffraction losses. For sufficiently small aperture Fresnel numbers N_0 the aperture diffraction losses can be estimated by first-order perturbation theory based upon the finite-N_m eigenfunctions (or upon the infinite-N_m functions renormalized to the finite-N_m amplitude at $r = 0$). The value of N_0 for which such first-order calculations are valid decreases rapidly as the Fresnel number N_m increases, because for large apertures the field distributions distort (higher-order perturbation theory) to avoid the aperture. This distortion occurs at approximately those values of N_0 and N_m for which an observer at one reflector, using light of the relevant wavelength and optics limited by the radius $r_m = N_m^{\frac{1}{2}}$, can resolve the aperture of radius $r_0 = N_0^{\frac{1}{2}}$ at the opposite reflector.[14]

VI. ACKNOWLEDGMENTS

I am grateful to W. L. Faust, C. G. B. Garrett, and R. A. McFarlane for suggesting the calculation of properties of perturbed cylindrical cavities, for discussions regarding the physical relevance of the results, and for comments concerning the preceding presentation. I am also grateful to T. Li and D. Slepian for references to the published literature and for several discussions correlating these results and methods with those of previous calculations.

APPENDIX

Reduction of Integral Equation (9) *to a Matrix Equation*

Truncating the series (13) after M terms and substituting the result into (9), we obtain[15] ($l = |l|$ in this Appendix)

$$\begin{aligned}
\kappa_{lp} g_{lp}(r) &= 2\pi \int_{r_0}^{r_m} dr'\, r' \sum_{m=1}^{M} \frac{(-1)^{m-1}(\pi r r')^{l+2(m-1)}}{(m+l-1)!(m-1)!}\, g_{lp}(r') \\
&= 2\pi \sum_{m=1}^{M} \frac{(-1)^{m-1}(\pi r)^{l+2(m-1)}}{(m+l-1)!(m-1)!} \\
&\quad \cdot \int_0^{r_m} dr'(r')^{l+2m-1}\, g_{lp}(r') \\
&= \left[\frac{(\pi r^2)^l}{l!}\right]^{\frac{1}{2}} \sum_{m=1}^{M} \frac{(-1)^{m-1}(\pi r^2)^{m-1}}{[(m-1)!(m+l-1)!/l!]^{\frac{1}{2}}} G_m(lp),
\end{aligned} \tag{32}$$

where

$$G_m(lp) \equiv \frac{2\pi}{[(m+l-1)!(m-1)!]^{\frac{1}{2}}} \cdot \int_{r_0}^{r_m} dr'\, r'(\pi r'^2)^{m-1+l/2} g_{lp}(r'). \tag{33}$$

Solving (32) for $g_{lp}(r)$ and substituting this expression into (33), we obtain after simple manipulations

$$\kappa_{lp} G_m(lp) = \sum_{k=1}^{M} \frac{(-1)^{k-1}}{[(m-1)!(m+l-1)!(k-1)!(k+l-1)!]^{\frac{1}{2}}} \times \frac{[(\pi N_m)^{l+m+k-1} - (\pi N_0)^{l+m+k-1}]}{(l+m+k-1)} G_k(lp). \tag{34}$$

We have used the definitions (7) to replace (r_0^2, r_m^2) by the Fresnel numbers (N_0, N_m).

Equation (34) is a matrix equation which must be solved for the eigenvalue κ_{lp} and for the M vector components $G_m(lp)$ appropriate to that eigenvalue. When these latter components are used in (32), one obtains the eigenfunction $g_{lp}(r)$ appropriate to the M-term truncation of (13). The normalization condition (10) on $g_{lp}(r)$ is equivalent to the condition

$$\kappa_{lp}\delta_{pq} = \sum_{m=1}^{M} (-1)^{m-1} G_m(lp) G_m(lq) \tag{35}$$

on the real vector components $G_m(lp)$. The sign condition $\mathrm{Re}\, g_{lp}(0^+) > 0$ becomes $G_1(lp) \geqq 0$ where, if $G_1(lp) = 0$, $G_2(lp) \leqq 0$, etc.

In programming the above equations for electronic-computer solution, one must insure that at each stage the computations maintain sufficient numerical accuracy. The relevance of this remark is clearly evident from the fact that, while the Bessel function $J_l(z)$ is of order unity for all real $z \geqq 0$, some terms of the series (13) will for $z \gg 1$ be of order $(e/2)^{2z}/2\pi z \gg 1$. That is, $J_l(z)$ will be the small difference of large numbers and care must be taken to insure that such small differences are accurately represented.

The program utilized to compute the results reported in this paper requires a nominal 0.0042 hr. of IBM 7094 running time to compute the M different eigenvalues and eigenvectors of (34) for $M = 20$. Timing for other values of M varies roughly as M^3.

REFERENCES

1. Fox, A. G., and Li, T., B.S.T.J., *40*, 1961, p. 453.
2. Patel, C. K. N., Faust, W. L., McFarlane, R. A., and Garrett, C. G. B., Appl. Phys. Letters, *4*, 1964, p. 18.

3. Boyd, G. D., and Gordon, J. P., B.S.T.J., *40*, 1961, p. 489.
4. Boyd, G. D., and Kogelnik, H., B.S.T.J., *41*, 1962, p. 1347.
5. Slepian, D., B.S.T.J., *43*, Nov., 1964, p. 3009.
6. Kogelnik, H., to be published in *Advances in Lasers*, ed. A. K. Levine.
7. Fox, A. G., Li, T., and Morgan, S. P., Appl. Opt., *2*, 1963, p. 544; Morgan, S. P., IEEE Trans. Microwave Theory and Techniques, *MTT-11*, 1963, p. 191; Kaplan, S., and Morgan, S. P., IEEE Trans. Microwave Theory and Techniques, *MTT-12*, 1964, p. 254; Newman, D. J., and Morgan, S. P., B.S.T.J., *43*, 1964, p. 113; and Cochran, J. Alan, B.S.T.J., *44*, Jan., 1965, p. 77.
8. She, C. Y., and Heffner, H., Appl. Opt., *3*, 1964, p. 703.
9. Bergstein, L., and Schachter, H., J. Opt. Soc. Am., *54*, 1964, p. 887. Cf. comments on this paper by Morgan, S. P., and Li, T., to be publ. in J. Opt. Soc. Am.
10. Goubau, G., and Schwering, F., IEEE Trans. Antennas and Propagation, *AP-9*, 1961, p. 248; Beyer, J. B., and Scheibe, E. H., IEEE Trans. Antennas and Propagation, *AP-10*, 1962, p. 349.
11. Erdelyi, A., et al., *Higher Transcendental Functions*, Vol. 2, New York, McGraw-Hill Book Co., 1953, pp. 188–192.
12. Li, T., to be published; cf. also Gloge, D., Arch. elektrischen Übertragung, *18*, 1964, p. 197.
13. Born, M., and Wolf, E., *Principles of Optics*, Pergamon Press, New York, 1959, pp. 394–397.
14. Faust, W. L., private communication.
15. Tricomi, F. G., *Integral Equations*, Interscience Publishers, Inc., New York, 1957, p. 55 ff.